

## Confinement effects on the low-field–high-field correspondences of hydrogenic impurity states in quasi-two-dimensional systems

J-P. Cheng and B. D. McCombe

*Department of Physics and Astronomy, State University of New York at Buffalo, Buffalo, New York 14260*

(Received 29 May 1990)

Correspondences between low- and high-magnetic-field quantum-number assignments for hydrogenic impurity states in quasi-two-dimensional systems have been established. The apparent discrepancy between the assignments for three-dimensional and two-dimensional systems for excited states can be understood in terms of two different limiting cases. Far-infrared magneto-optical measurements have been carried out on well-center-doped Si donors in GaAs/Al<sub>0.3</sub>Ga<sub>0.7</sub>As multiple quantum wells with relatively narrow well width; the results show two-dimensional behavior, in agreement with the predictions in this well-width and magnetic-field region.

Magnetic-field effects on shallow-impurity (hydrogen-like) states in semiconductors have been the subject of wide interest for many years. Due to the absence of exact solutions for this problem, certain approximations have been made at low and high magnetic fields; thus the correspondence of energy states between the low-field and high-field limits has attracted considerable attention. For three-dimensional (3D) systems, such correspondences have been established after years of theoretical and experimental effort.<sup>1–5</sup> Numerical calculations have been developed based on symmetry discussions.<sup>6,7</sup> For a strictly two-dimensional (2D) system, the situation is much simpler due to the removal of one degree of freedom. The correspondences can be established with no ambiguity.<sup>8</sup> However, the assigned correspondence for excited states shows an apparent discrepancy with the three-dimensional results. For example, 2D calculation predicts that the  $3p_{+1}$  state in the low-field limit with the usual hydrogen-atom notation should correspond to the  $N=2$  Landau level in the high-field limit, while it is associated with the  $N=1$  Landau level in the 3D case, as has been confirmed by experiments.<sup>9</sup> This “dimensionality-dependent” behavior has motivated us to study quasi-two-dimensional systems, in which neither theoretical calculation nor detailed experimental investigation has been carried out for the higher excited impurity states (such as  $3p_{\pm 1}$  and  $4p_{\pm 1}$ ) in the presence of an external magnetic field. In principle, the 2D and 3D results can be reached by taking the limit of the confinement length going to zero and infinity for infinite potential barriers on the results of a quasi-2D system, respectively.

Within the effective-mass approximation, the Hamiltonian of a quasi-2D hydrogen impurity in a uniform and static external magnetic field along the direction of confinement (chosen as  $\hat{z}$ ) has the general form

$$H = \frac{\mathbf{p}^2}{2m^*} - \frac{e^2}{\epsilon r} + \frac{1}{2}\omega_c L_z + \frac{1}{8}m^*\omega_c^2(x^2 + y^2) + V(z), \quad (1)$$

where we have chosen the symmetric gauge,  $e$  and  $m^*$  are the charge and effective mass of the electron,  $\epsilon$  is the dielectric constant of the semiconductor,  $L_z$  is the  $z$  com-

ponent of angular momentum, and  $\omega_c = eB/m^*c$  is the cyclotron frequency. Without loss of generality, the confinement potential can be chosen as

$$V(z) = \begin{cases} \infty, & |z| \geq W/2 \\ 0, & |z| < W/2, \end{cases} \quad (2)$$

which implies that the impurity is doped at the center of the well with well width  $W$ . It is obvious that the  $z$  component of angular momentum and the parity along  $z$ ,  $P(z)$ , are conservative throughout the discussion.

In the absence of a magnetic field and in the 3D limit ( $B=0$ ,  $a_B \ll W$ , where  $a_B = \hbar^2\epsilon/m^*e^2$  is the effective Bohr radius), the zeroth-order solutions of the Hamiltonian of Eq. (1) are just those of the usual 3D hydrogen atom. The quantum numbers are  $(n, l, m)$ , and the zeroth-order eigenenergies are

$$E_{nlm}^0 = -R/n^2, \quad n = 1, 2, 3, \dots, \quad (3)$$

where  $R = e^2/2\epsilon a_B$  is the effective Rydberg. The wave function of state  $(n, l, m)$  has  $(n-l-1)$  nodal spheres and  $(l-|m|)$  nodal cones along the  $z$  direction. Parity under the transformation  $z \rightarrow -z$  is odd or even according to whether  $P(z) = (-1)^{l-|m|}$  is  $-1$  or  $+1$ , respectively. On the other hand, in the presence of a strong confining potential  $V(z)$  at zero field ( $B=0$ ,  $W \ll a_B$ ), it is convenient for future discussion to rewrite the Hamiltonian as

$$H = \left[ \frac{1}{2m^*} (p_x^2 + p_y^2) - \frac{e}{\epsilon\rho} \right] + \left[ \frac{1}{2m^*} p_z^2 + V(z) \right] + H', \quad (4)$$

with  $\rho = (x^2 + y^2)^{1/2}$  and  $H' = (e^2/\epsilon)(1/\rho - 1/r)$ , which is a perturbation on the 2D limit. The term in the first set of large parentheses is the Hamiltonian for a strictly 2D hydrogen atom and can be analytically solved. Thus the problem of a strongly confined hydrogenic impurity can be treated as a 2D hydrogen atom plus an associated sub-band structure with an additional perturbation term.

The quantum numbers for the unperturbed Hamiltonian now become  $(\bar{n}, m, i)$  with  $(\bar{n}, m)$  denoting the eigenstates of the 2D hydrogen atom and  $i$  the subband index. The zeroth-order energy eigenvalues are given by

$$E_{\bar{n}mi}^0 = -R / (\bar{n} - \frac{1}{2})^2 + E_i, \quad \bar{n}, i = 1, 2, 3, \dots \quad (5)$$

The wave functions have  $(\bar{n} - |m| - 1)$  nodal cylinders and  $(i - 1)$  nodal planes along the  $z$  direction. Parity along  $z$  is odd or even according to whether  $P(z) = (-1)^{i-1}$  is  $-1$  or  $+1$ , respectively. The confinement in the  $z$  direction has condensed the nodal cones into planes parallel to the  $x$ - $y$  plane, whereas it hardly affects the properties in the  $x$ - $y$  plane. With the concept of nodal surface conservation, the correspondence between 3D and 2D limiting cases at zero magnetic field can be set up as

$$\begin{aligned} n - l - 1 &\leftrightarrow \bar{n} - |m| - 1, \\ l - |m| &\leftrightarrow i - 1. \end{aligned} \quad (6)$$

The second relation also has ensured parity conservation in the  $z$  direction when  $V(z)$  has reflection symmetry. The correspondence for several low-lying energy states are listed in Table I (under low field). In this table, the standard spectroscopic notation (e.g.,  $1s$ ,  $2p_{\pm 1}$ , etc.) has been used to denote the 3D hydrogenic states, whereas  $(\bar{n}, m, i)$  are used to label the states in the 2D limit.

Physically, the confinement removes some of the degeneracies by pushing states with larger wave-function extension in the  $z$  direction to higher energies. The states with  $|m| = l$  have the smallest extension along  $\hat{z}$  among those states with the same  $n$  and  $l$ , and thus belong to the ground subband in quasi-2D systems. The one-to-one correspondences of Eq. (6) allow one to label the quasi-2D impurity states with the 3D atomic notation. This has come into common usage without formal justification; however, it is worth emphasizing that such labeling is nothing more than an indication of the bulk parentage, which can be tracked back from the quasi-2D states by continuously reducing confinement. The spectroscopic notation has been used to label the strictly 2D hydrogenic states<sup>8</sup> by defining  $l = |m|$ . For a quasi-2D system such notation may produce ambiguity (e.g., the  $2p_0$  state in the 3D atomic notation is the  $1s$  state of the second subband in the 2D notation).

At high magnetic fields, but still in the strong confinement limit ( $R \ll \hbar\omega_c \ll \Delta E_i$ , where  $\Delta E_i$  is the subband separation), the Coulomb term ( $-e^2/\epsilon r$ ) in Eq. (1) can be treated as a perturbation. Three quantum numbers that completely describe the system in this case are  $(N, m, i)$ , and the zeroth-order energies are given by

$$\begin{aligned} E_{Nmi}^0 &= (N + \frac{1}{2})\hbar\omega_c + E_i, \\ N &= 0, 1, 2, \dots, \quad i = 1, 2, \dots, \end{aligned} \quad (7)$$

where  $N$  is the Landau index and  $m \leq N$ . The perturbation term becomes important in this problem only when two states with the same  $m$  and  $P(z)$  attempt to cross each other as the magnetic field is varied, since the perturbation has spherical symmetry. This cannot happen in the 2D limiting case ( $\Delta E_i \rightarrow \infty$ ); hence, the correspon-

TABLE I. Correspondence between quasi-2D  $(\bar{n}, m, i)$  and 3D  $(n, l, m)$  eigenstates at zero magnetic field [the spectroscopic notations are used to denote  $(n, l, m)$ ] and their corresponding Landau levels at high magnetic field in both 2D and 3D limits for several energy levels.

Quasi-2D $(\bar{n}, m, i)$	3D bulk $(n, l, m)$	High field	
		2D limit $N$	3D limit $N$
(1,0,1)	$1s$	0	0
(2,0,1)	$2s$	1	0
(2,+1,1)	$2p_{+1}$	1	1
(2,-1,1)	$2p_{-1}$	0	0
(2,0,2)	$2p_0$	0	0
(3,+1,1)	$3p_{+1}$	2	1
(3,-1,1)	$3p_{-1}$	1	0
(4,+1,1)	$4p_{+1}$	3	1
(4,-1,1)	$4p_{-1}$	2	0

dence between low-field states  $(\bar{n}, m, i)$  and high-field states  $(N, m, i)$  can be determined with no ambiguity.<sup>8</sup> If we again make use of the concept of nodal surface conservation, the result is

$$\bar{n} - |m| - 1 \leftrightarrow N - \frac{1}{2}(m + |m|), \quad (8a)$$

or equivalently,

$$N \leftrightarrow (\bar{n} - 1) + \frac{1}{2}(m - |m|). \quad (8b)$$

This is exactly the same as the result of Ref. 8, where no crossing between two states with the same  $m$  for a strictly 2D hydrogen atom was considered. It is obvious that the strictly 2D case is just the limit  $\Delta E_i \rightarrow \infty$ , so that only the ground subband  $E_1$  is occupied in a quasi-2D system.

On the other hand, when the confinement is relaxed by letting  $W$  become so large that  $\Delta E_i \sim R \ll \hbar\omega_c$ , the states with smaller  $i$  but larger  $N$  will cross states with larger  $i$  and smaller  $N$  if the Coulomb term is neglected. However, such crossing is not allowed between states having the same  $m$  and  $P(z)$  due to the nonvanishing off-diagonal matrix elements of the Coulomb term, which should not be treated as a perturbation in this case. For example,  $3p_{+1}$  ( $\bar{n}=3$ ,  $m=1$ ,  $i=1$ ) will cross  $3d_{+1}$ ,  $4f_{+1}$ ,  $5g_{+1}$ , and so on ( $\bar{n}=2$ ,  $m=1$ ,  $i=2,3,4, \dots$ , respectively), if the Coulomb term is neglected, since  $3p_{+1}$  has a larger slope ( $N=2$ ) in energy versus magnetic field than  $3d_{+1}$ ,  $4f_{+1}$ , and  $5g_{+1}$  ( $N=1$ ). When the Coulomb term is turned on, the crossing is prevented for certain states (it may cross  $3d_{+1}$  if parity is a good quantum number, but not  $4f_{+1}$ ), and  $3p_{+1}$  is depressed and eventually approaches a slope equal to that of the upper energy states ( $N=1$ ). This is like a typical anti-level-crossing process, except that the upper branch does not approach the slope of the lower-energy level ( $N=2$ ) because of interaction with even higher-energy states. In fact, the Coulomb term mixes all states with the same  $m$  (but different  $N$  and  $i$ ) and forces all of them to move along with the lowest allowed Landau level for that particular  $m$ . That is,

$$\text{all } m \leq 0 \leftrightarrow N = 0, \quad (9a)$$

$$\text{all } m > 0 \leftrightarrow N = m. \quad (9b)$$

These are the well-known 3D correspondence rules.<sup>9</sup> Equations (8) and (9) are tabulated for several states in Table I (under high field). It is easy to see that differences between 2D and 3D will occur for states like  $2s$ ,  $3p_{\pm 1}$ ,  $4p_{\pm 1}$ , and so on, but not for states like  $1s$ ,  $2p_{\pm 1}$ ,  $2p_0$ , and so on. Thus confinement effects play a crucial role in understanding naturally the apparent “discrepancy” between the 2D and 3D correspondences.

It is clear from the above discussion that experimental investigations of those states with qualitatively different behavior in the high field between 3D and 2D systems (such as  $3p_{+1}$  and  $4p_{+1}$ ) are crucial to verify the correspondences between low and high magnetic fields. Far-infrared magneto-optical measurements of intra-impurity transitions for well-center (central  $\frac{1}{3}$ )-doped Si donors ( $N_D = 1 \times 10^{16} \text{ cm}^{-3}$ ) in GaAs/Al<sub>0.3</sub>Ga<sub>0.7</sub>As multiple-quantum-well structures have been carried out on two samples with different well widths (sample No. 1, 125 Å; and sample No. 2, 150 Å) at liquid-helium temperature and magnetic fields up to 9 T. The subband separations ( $E_2 - E_1$ ) are about 550 and 420  $\text{cm}^{-1}$  for sample No. 1 and sample No. 2, respectively, much larger than the cyclotron frequency ( $\sim 120 \text{ cm}^{-1}$  at 9 T). A low-frequency ( $\sim 100 \text{ Hz}$ ) capacitively coupled photoconductivity technique was used to enhance the signal-to-noise ratio. All measurements were made with a slow-scan (repetitively scanned) Fourier-transform spectrometer with far-infrared (FIR) light propagation parallel to the magnetic field and field normal to the sample surface (Faraday geometry).

Figure 1 shows the photoconductivity spectra for sam-

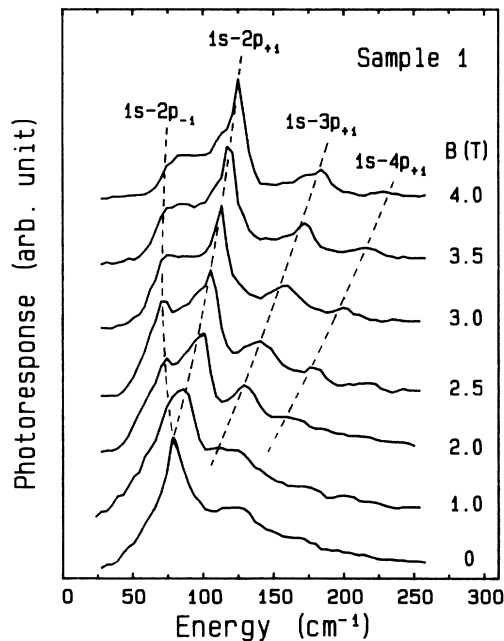


FIG. 1. Capacitively coupled photothermal ionization spectra for impurity transitions on sample No. 1 at  $T \approx 4.2 \text{ K}$  and several magnetic fields. The “shoulder” at  $\sim 120 \text{ cm}^{-1}$  in the zero-field spectrum is an artifact from the interference of white polyethylene window, not the  $1s \rightarrow 3p_{+1}$  or  $1s \rightarrow 4p_{+1}$  transition.

ple No. 1 at several magnetic fields. At zero field, the most prominent feature is the strong peak at  $\sim 78 \pm 1 \text{ cm}^{-1}$ , which has been identified as  $1s \rightarrow 2p_{\pm 1}$  transitions degenerate at  $B=0$ . This strong line is split into  $1s \rightarrow 2p_{-1}$  and  $1s \rightarrow 2p_{+1}$  peaks as the field increases, and their behavior is well known.<sup>10,11</sup> Unfortunately, these transitions cannot yield information concerning the correspondences since both initial and final states exhibit no difference between 3D and 2D. In addition to these strong features, there are two more weaker lines at higher frequencies. They move to higher frequencies much more rapidly in comparison with  $1s \rightarrow 2p_{+1}$  as the magnetic field increases.

To identify these transitions, the selection rules have to be examined. In the geometry of these experiments, the electric field of the FIR light is in the  $x$ - $y$  plane. The electric-dipole-allowed transitions are  $\Delta m = \pm 1$  and  $\Delta P(z) = 0$ . At low temperature, the initial state is the ground state  $1s$  [or (101) in the quasi-2D low-field notation]. The transition energies are much lower than the subband separation at this well width, indicating that they are intra-subband transitions. Considering additionally the slopes of the transition energies as a function of field discussed below, we identify these transitions (in the 3D atomic notation) as  $1s \rightarrow 3p_{+1}$  and  $1s \rightarrow 4p_{+1}$ . It is worthwhile to point out that we cannot exclude the  $1s \rightarrow 4p_{-1}$  transition (accompanying  $1s \rightarrow 3p_{+1}$ ) and  $1s \rightarrow 5p_{-1}$  transition (accompanying  $1s \rightarrow 4p_{+1}$ ) as possibilities from the above selection rules. However, their intensity should be much weaker due to smaller dipole transition matrix elements. We exclude them on this basis.

In Fig. 2, we plot the transition energies as a function of magnetic field for two samples, solid squares are for sample No. 1, and open circles are for sample No. 2. At

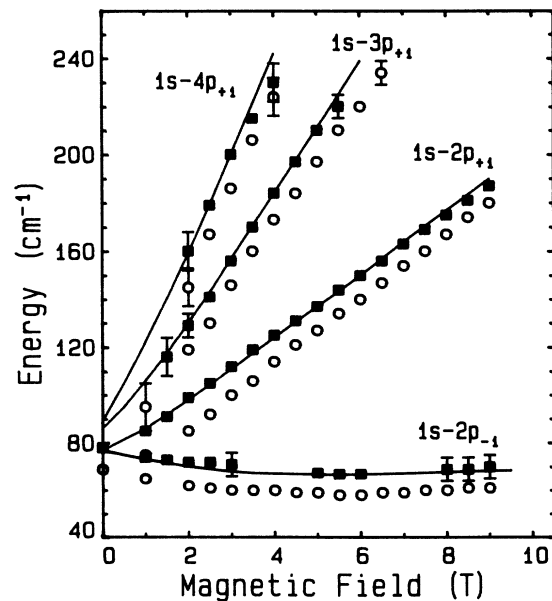


FIG. 2. Magnetic-field dependence of impurity transitions on two well-center-doped multiple-quantum-well samples; solid squares are for sample No. 1 (125-Å well) and open circles for sample No. 2 (150-Å well). Lines are rough fits (see text).

present, theoretical calculations for  $1s \rightarrow 3p_{+1}$  and  $1s \rightarrow 4p_{+1}$  transitions in this system are not available to compare with our experimental data. For a rough comparison, the curves in Fig. 2 are calculated from the simple formula

$$E_k = E(1s \rightarrow 2p_{-1}) + k\hbar\omega_c + \Delta_k, \quad (10)$$

where  $E(1s \rightarrow 2p_{-1})$  is the transition energy for  $1s \rightarrow 2p_{-1}$  in a magnetic field, calculated by Greene and Bajaj<sup>10</sup> with well width 125 Å (sample No. 1),  $\hbar\omega_c = 13.7 \text{ cm}^{-1}/\text{T}$  (nonparabolicity is ignored here),  $k=0,1,2,3$  corresponding to  $1s \rightarrow 2p_{-1}$ ,  $2p_{+1}$ ,  $3p_{+1}$ , and  $4p_{+1}$ , respectively.  $\Delta_k$  is the parameter indicating the transition-energy differences at  $B=0$  relative to the  $1s \rightarrow 2p_{-1}$  transitions. In spite of the roughness of this formulation, these curves fit the data reasonably well. It is apparent that  $1s \rightarrow 3p_{+1}$  has a slope of  $\sim 2\hbar\omega_c$  and  $1s \rightarrow 4p_{+1}$  has a slope of  $\sim 3\hbar\omega_c$  in the high-field region. Data taken on

sample No. 2 show exactly the same qualitative behavior as sample No. 1, except that the transition energies are lower due to the larger well width. Experimental results clearly indicate that states  $3p_{+1}$  and  $4p_{+1}$  move with  $N=2$  and  $N=3$  in the high-magnetic-field region, respectively, since  $1s$  moves with  $N=0$ . The correspondences between the low-field and high-field states  $(N, m, i)$  are  $3p_{+1} \leftrightarrow (2, 1, 1)$  and  $4p_{+1} \leftrightarrow (3, 1, 1)$ , respectively, which are apparently different from the results of bulk<sup>4-7,9</sup> and in agreement with 2D predictions in previous discussions (see Table I), as expected in this well width and magnetic-field region ( $\Delta E_i \gg \hbar\omega_c \gg R$ ).

We are grateful for the expert molecular-beam-epitaxy growth of the samples used in the measurements by J. Ralston, G. Wicks, and W. Schaff of Cornell University. This work was supported in part by the Office of Naval Research under Grant No. N00014-89-J-1673.

<sup>1</sup>R. J. Elliott and R. Loudon, *J. Phys. Chem. Solids* **15**, 196 (1960).

<sup>2</sup>W. S. Boyle and R. E. Howard, *J. Phys. Chem. Solids* **19**, 181 (1961).

<sup>3</sup>H. C. Praddaude, *Phys. Rev. A* **6**, 1321 (1972).

<sup>4</sup>S. Narita and M. Miyao, *Solid State Commun.* **9**, 2161 (1971).

<sup>5</sup>R. J. Wagner and B. D. McCombe, *Phys. Status Solidi B* **64**, 205 (1974).

<sup>6</sup>C. Aldrich and L. Greene, *Phys. Status Solidi B* **93**, 343 (1979).

<sup>7</sup>P. C. Makado and N. C. McGill, *J. Phys. C* **19**, 873 (1986).

<sup>8</sup>A. H. MacDonald and D. S. Ritchie, *Phys. Rev. B* **33**, 8336 (1986).

<sup>9</sup>For recent work, see, e.g., C. J. Armistead, R. A. Stradling, and Z. Wasilewski, *Semicond. Sci. Technol.* **4**, 557 (1989).

<sup>10</sup>Ronald L. Greene and K. K. Bajaj, *Phys. Rev. B* **31**, 6498 (1985).

<sup>11</sup>See, e.g., N. C. Jarosik, B. D. McCombe, B. V. Shanabrook, J. Comas, John Ralston, and G. Wicks, *Phys. Rev. Lett.* **54**, 1283 (1985).